

“© 2011 IEEE. Personal use of this material is permitted. Permission from IEEE must be obtained for all other uses, in any current or future media, including reprinting/republishing this material for advertising or promotional purposes, creating new collective works, for resale or redistribution to servers or lists, or reuse of any copyrighted component of this work in other works.”

Semi-autonomous Wheelchair Developed Using a Unique Camera System Configuration Biologically Inspired by Equine Vision

Jordan S. Nguyen, Yvonne Tran, Steven W. Su, Hung T. Nguyen, *Senior Member, IEEE*

Abstract—This paper is concerned with the design and development of a semi-autonomous wheelchair system using cameras in a system configuration modeled on the vision system of a horse. This new camera configuration utilizes stereoscopic vision for 3-Dimensional (3D) depth perception and mapping ahead of the wheelchair, combined with a spherical camera system for 360-degrees of monocular vision. This unique combination allows for static components of an unknown environment to be mapped and any surrounding dynamic obstacles to be detected, during real-time autonomous navigation, minimizing blind-spots and preventing accidental collisions with people or obstacles. This novel vision system combined with shared control strategies provides intelligent assistive guidance during wheelchair navigation and can accompany any hands-free wheelchair control technology. Leading up to experimental trials with patients at the Royal Rehabilitation Centre (RRC) in Ryde, results have displayed the effectiveness of this system to assist the user in navigating safely within the RRC whilst avoiding potential collisions.

I. INTRODUCTION

PHYSICAL mobility impairment, in many cases, can result in fewer socializing and leisure opportunities, decreased pursuits of goals, loss of physical independence, and heightened risk of depression in sufferers. Mobility aids, such as electric-powered wheelchairs, can provide significant improvements to the quality of life for many people living with physical disability. However, safe control of conventional powered wheelchairs require from the user significant levels of skill, attention, and judgment [1]. Accidents are a potential risk when using wheelchairs and can cause injuries if they occur. For example, in the United States around 85,000 serious wheelchair accidents occur annually, with the trend being expected to increase [2].

Recent decades have seen great advancements in the development of autonomous and semi-autonomous powered wheelchairs. Some popular examples of these ‘smart wheelchair’ advancements, featuring shared-control

strategies developed for various wheelchair platforms include *SENA* [3], *Rolland* [4], *Hephaestus* [5], and *Navchair* [6]. However, these wheelchairs do not facilitate operation in unknown dynamic environments, either requiring prior knowledge about the environment or having no capacity for combining with data about the local environment. Furthermore, these systems require further development before being capable of real-time operation.

Robotics techniques play a large role in intelligent system design such as smart wheelchairs. Many modern artificial sensors used in intelligent robotic applications are biologically inspired and modeled on real sensors in living systems such as humans, animals, and insects [7]. In this paper, we present a semi-autonomous wheelchair system that utilizes a novel combination of both stereoscopic and spherical vision cameras in a manner that has been inspired by the equine visual system.

Horses in nature spend approximately 50-60% of their time grazing with their heads lowered and eyes near ground level. This leaves them vulnerable to predation from such threats as wolves, lions, and snakes. However, horses inherently have a large range of vision which provides early warning of approaching, and potentially threatening, dynamic movements outside of their binocular vision range. This allows for quick instinctual assessment of the local environment and a speedy escape from imminent danger [8].

Similarly, the wheelchair’s vision system being modeled on this allows for the stereoscopic vision to map static objects ahead of the wheelchair in real-time and use obstacle avoidance strategies for both static and dynamic objects. The spherical vision, in addition, provides dynamic obstacle detection all around the wheelchair, preventing collisions with moving objects which have not already been mapped.

This wheelchair is aimed at assisting people with severe disabilities, and is able to interface with any hands-free control technology, such as brain-computer interfaces. Through the design of multivariable control strategies, the wheelchair provides automated guidance assistance and obstacle avoidance, allowing safe navigation to assist hands-free control. Experiments were conducted to assess the performance of the designed vision configuration and automated guidance system within the RRC in Sydney, leading up to experimental trials with tetraplegic patients from the centre.

In Section II of this paper, the biologically inspired wheelchair vision configuration and design is provided. Section III presents results and discussions of the designs and real-time performance of the overall designed system at the RRC, incorporating multivariable control and automated guidance assistance. Section IV concludes this paper.

This work was supported in part by Australian Research Council under Discovery Grant DP0666942 and LIEF Grant LE0668541.

Jordan S. Nguyen is with the Faculty of Engineering and Information Technology, University of Technology, Sydney, Broadway, NSW 2007, Australia (phone: +612-9514-4441; fax: +61 2 9514 2868; e-mail: Jordan.S.Nguyen@eng.uts.edu.au).

Yvonne Tran is with the Faculty of Engineering and Information Technology, University of Technology, Sydney, Broadway, NSW 2007, Australia (e-mail: Yvonne.Tran@uts.edu.au).

Steven W. Su is with the Faculty of Engineering and Information Technology, University of Technology, Sydney, Broadway, NSW 2007, Australia (e-mail: Steven.Su@uts.edu.au).

Hung T. Nguyen is with the Faculty of Engineering and Information Technology, University of Technology, Sydney, Broadway, NSW 2007, Australia (e-mail: Hung.Nguyen@uts.edu.au).

II. DESIGN AND DEVELOPMENT

A. Biological Inspiration – Equine Visual System

The equine eye is large and prominent, being housed within enclosed orbits located laterally in the skull [9]. Using measurements based on the position and dimensions of the equine eye, the retinal field of view of each eye in the vertical plane has been estimated to be about 178° [10], whilst that in the horizontal plane is slightly greater, being about 200° [11]. The horizontally elongated pupil in the equine eye facilitates wider lateral vision than, for example, the circular pupil of the human eye [12].

The binocular overlap of the visual field is located down the nose of the horse and has been found to have a width of around 65° [13]. Two blind spots have been identified within the equine visual field, being one in front of the forehead, and one (approximately 25°) directly behind the horse [12]. Visual field characteristics and the extent of blind spots do vary between different horse breeds [14], however the overall ideas of the equine visual system have been a sufficient inspiration for the vision system developed in the semi-autonomous wheelchair described in this paper.

The novel combination of stereoscopic cameras and spherical vision cameras mimics the binocular and monocular fields of view inherent in the equine visual system, whilst also minimizing the blind spots (Fig. 1).

The stereoscopic cameras at the front of the wheelchair provide approximately 66° of vision similar to the binocular vision of a horse, and the spherical vision cameras above the back of the wheelchair provide complete 360° monoscopic vision, similar to the monocular vision of the horse without the posterior blind spots. This allows 3D mapping of the local environment ahead of the wheelchair and detection of obstacles posing as potential collision dangers (dynamic in particular) all around the wheelchair.

B. Stereoscopic Vision

The Point Grey Research (PGR) company's Bumblebee XB3 stereoscopic camera system was used for this project. The purpose of stereo vision is to perform range measurements based on the left and right images obtained from stereoscopic cameras. An algorithm is implemented to establish the correspondence between image features in different views of the scene and then calculate the relative displacement between feature coordinates in each image. In order to produce a disparity image, the Sum of Absolute

Differences (SAD) correlation algorithm in Eq.1 is used to compare a neighborhood in one stereo image to a number of neighborhoods in the other stereo image [15],

$$SAD = \min_{d=d_{\min}}^{d_{\max}} \sum_{i=-M}^{+M} \sum_{j=-M}^{+M} |I_R(x+i, y+j) - I_L(x+i+d, y+j)|, \quad (1)$$

where a window of size $(2M+1) \times (2M+1)$ (correlation mask) is centered at the coordinates of the matching pixels (i, j) , (x, y) in one stereo image, I_L and I_R are the intensity functions of the left and right images, and d_{\min} , d_{\max} are the minimum and maximum disparities. The disparity d_{\min} of zero pixels often corresponds to an infinitely far away object and the disparity d_{\max} denotes the closest position of an object. The disparity range was tuned to between 0.5m and 5m from the front of the cameras which provided adequate mapping accuracy and distance for response to obstacles.

Once a disparity image is produced from the processed left and right camera images, a 3D point map can be created which maps the depth-determined pixels from the disparity image into a 3D plane. These are then sorted into 3 arrays representing each pixel's (x, y, z) coordinates. The depth mapping program utilizes this data and maps the placement of objects in the wheelchair's local environment, relative to the wheelchair, allowing information such as object distances from the wheelchair and upcoming gap widths to be known. Wheel encoders are also utilized to calculate and reposition static features in the map once they move out of sight of the stereoscopic vision as previously design in [15].

C. Spherical Vision

PGR's Ladybug2 Spherical Digital Video Camera System has six closely-packed Sony 1024x768 CCD 0.8 Mega Pixel (MP) cameras that enable the system to collect image data from more than 80% of the full sphere, and an IEEE-1394b interface that allows streaming to disk at up to 30 frames-per-second (fps). [16]

The Ladybug2 camera configuration (Fig. 2) consists of five cameras around and one on top to allow for complete 360° spherical vision around and above the system. This is useful in this project for detecting obstacles located within the safety zones of the wheelchair which may obstruct movement or rotation in the corresponding directions.

The wheelchair was taken to the Ryde RRC for data gathering in the environment the wheelchair is intended to be trialed in by tetraplegic patients (Fig. 3). This environment is constantly changing based on cleaners'

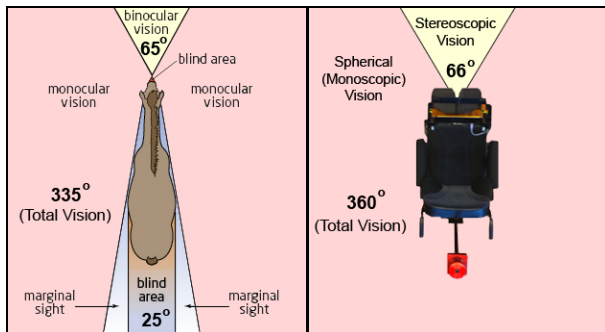


Fig. 1: Visual System of a Horse (left); Wheelchair Vision Design (right)

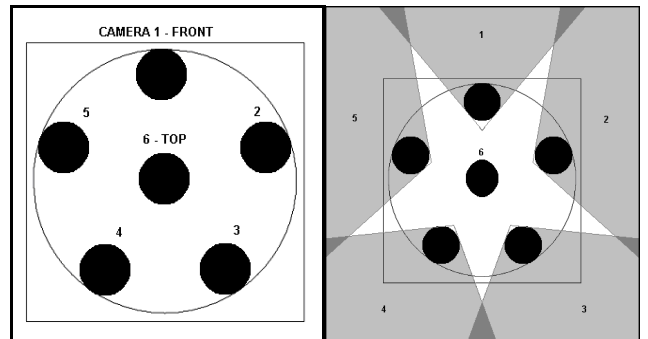


Fig. 2: Ladybug 2 Top-view Layout Diagram and Camera Range Zones



Fig. 3: Photos of Wheelchair Trial Sites at the Ryde Royal Rehab Centre

trolleys, bins, and general objects being moved around in the hallways and rooms (Fig. 3). To allow for flexibility in navigation, environments are being treated as unknown, so the wheelchair needs to be able to both map static objects as well as detect dynamic obstacles such as people who walk around in the RRC.

III. RESULTS

A. Performance of Stereoscopic Vision Mapping

When taken to the RRC, the stereoscopic cameras were calibrated to the environmental lighting conditions present. As previously designed [15], the conversion from stereoscopic images to disparity map to 3D depth map creation had been optimized, so once calibrated the cameras effectively mapped the placement of objects in the local environment. The distance to common objects seen in the RRC were measured and distances varied to compare against the depth calculation results to those objects (Table. 1). Results showed the further away objects were placed from the wheelchair up to 5m, the higher the error in many cases. However the results were still very useful, showing in the range of vision up to 5m a maximum error of $\pm 6\text{cm}$.

Observation of the depth maps combined with odometry changes, using the wheel encoders as previously designed [16], showed accurate repositioning of obstacle depth data once they had moved outside the stereoscopic vision range. This recalculated data is then verified and information added from the real-time classification of spherical camera images taken all around the wheelchair.

B. Performance of Spherical Vision Obstruction-Detection

The task involved here is to determine whether or not obstacles are obstructing movements of the wheelchair in any direction through determining which of the 4 surrounding camera images contain objects in close proximity. These are cameras 2-5 (Fig. 2, Fig. 4), as vision in camera 1 is obstructed by the person and features of the wheelchair. This data is used for the decision-making process involved in autonomously moving the wheelchair whilst avoiding moving and rotating into objects. This is

| Actual (m) | Wall | Door | Garbage Bin | Fire Hydrant | Wheelchair | Cleaner | Trolley |
|------------|-----------|-----------|-------------|--------------|------------|-----------|-----------|
| 0.5 | 0.50±0.02 | 0.50±0.02 | 0.50±0.02 | 0.50±0.02 | 0.50±0.01 | 0.50±0.02 | 0.50±0.02 |
| 1 | 1.00±0.02 | 1.00±0.02 | 1.00±0.02 | 1.02±0.02 | 1.00±0.02 | 1.00±0.02 | 1.00±0.02 |
| 1.5 | 1.50±0.02 | 1.50±0.02 | 1.50±0.03 | 1.52±0.03 | 1.50±0.03 | 1.50±0.03 | 1.50±0.03 |
| 2 | 2.00±0.03 | 2.00±0.03 | 2.00±0.03 | 2.01±0.03 | 2.00±0.03 | 2.00±0.03 | 2.00±0.03 |
| 2.5 | 2.49±0.01 | 2.49±0.04 | 2.49±0.03 | 2.52±0.02 | 2.50±0.02 | 2.49±0.02 | 2.50±0.03 |
| 3 | 2.98±0.03 | 2.98±0.04 | 3.02±0.02 | 3.05±0.01 | 3.01±0.02 | 3.00±0.02 | 3.01±0.03 |
| 3.5 | 3.48±0.03 | 3.48±0.02 | 3.52±0.03 | 3.53±0.03 | 3.48±0.02 | 3.51±0.01 | 3.52±0.04 |
| 4 | 3.98±0.03 | 4.02±0.03 | 3.99±0.03 | 4.02±0.03 | 3.97±0.03 | 4.01±0.03 | 4.02±0.04 |
| 4.5 | 4.47±0.03 | 4.48±0.04 | 4.48±0.03 | 4.59±0.05 | 4.48±0.03 | 4.52±0.04 | 4.51±0.03 |
| 5 | 4.99±0.04 | 4.99±0.05 | 4.98±0.02 | 5.00±0.06 | 5.00±0.04 | 5.01±0.03 | 4.99±0.05 |

Table 1: Stereoscopic Cameras: Object Estimated vs Actual Distances(m)

mainly used to avoid turning into people or objects, and the process of determining whether or not there are obstructions to rotation is achieved through Neural Network (NN) classification of individual, instantaneous camera images. The NN created for this purpose is two-layer, utilizing a generalized Delta Learning Rule for Error Back Propagation Training. This gives two output neurons, representing Free-space and Obstacle-obstruction as the two possible classes.

Various images from all 4 cameras were acquired individually and a single classification system was created for all. Once an image has been acquired as 8-bit grey-scale, it undergoes preprocessing which includes resolution adjustment (lowering resolution of each image to 53x53pixels) for faster image processing, adjustment of brightness, gamma, and contrast settings to improve visibility of objects, closing and smoothing of the image, Prewitt edge-detection, and finally applying a threshold to the image to convert it to a binary edge-detected image. This superimposed on the original 53x53 grey-scale image and pixel-flattened into a single column input matrix provides both image intensity information as well as enhanced edge-detected information, improving on previous designs [16].

The classification system was setup with 180 training images, 180 validation images, and 180 test images (90 of each set from images with obstructions and 90 of each set from images with free-space). The training process optimizes the configuration to produce highest accuracies possible whilst retaining stability in the system.

The results for this trial produced an optimal number of 6 hidden neurons for the Neural Network (Fig. 4), a Learning Constant of 0.024, and a Momentum Constant of 0.019. Overall accuracies were optimized to 98.89%, with a sensitivity of 97.83% and a specificity of 100% (Table. 2). These results show this classification method can be used effectively to help aid in the decision-making process of the automated guidance system in the semi-autonomous wheelchair. A real-time graphical user interface (GUI) shows classifications as they occur, with red lights indicating detected obstructions (Fig. 5).

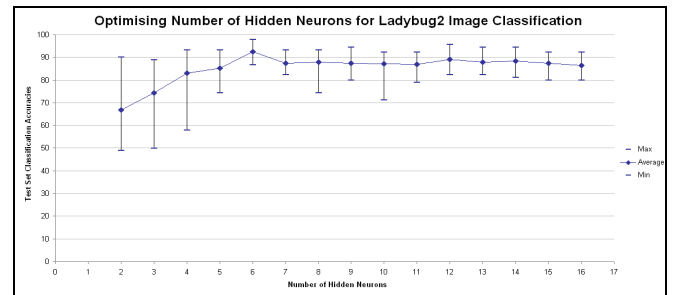


Fig. 4: Neural Network Hidden Neuron Optimization

| CLASS | Results | | Test Samples | Accuracy |
|-------------|--------------------|---------------------|--------------|----------|
| | True-Positive (TP) | False-Positive (FP) | | |
| Obstruction | 90 | 0 | 90 | 100% |
| Free-space | 88 | 2 | 90 | 97.78% |

| ANALYSIS | | |
|------------------|----------------------|--------|
| Sensitivity | TP/(TP+FN) | 97.83% |
| Specificity | TN/(TN+FP) | 100% |
| Overall Accuracy | (TP+TN)/TotalSamples | 98.89% |

Table 2: Optimised Neural Network Results

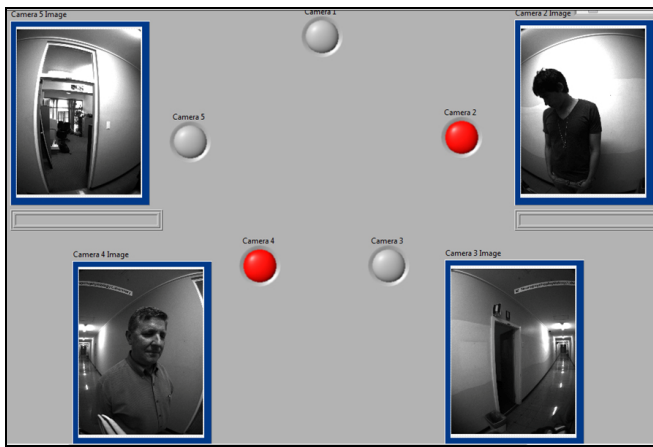


Fig. 5: Ladybug2 Image Classification Results – Obstructions Detected

C. Performance of Wheelchair Navigation in the RRC

The automated navigation system of the wheelchair, utilizing concepts of enhanced Vector Polar Histogram (VPH+) [17] for obstacle avoidance, was tested in the corridors at the RRC for the purpose of assessing this system's performance leading up to patient trials. Starting at the front entrance of Rehabilitation Studies Unit, the wheelchair had to navigate around corners and down the stretch of a corridor with both static and dynamic obstacles present. The stereoscopic cameras mapped the unknown local environment (with random lighting conditions) as the wheelchair navigated, and the mapping results were recorded for this test (white mapping points in Fig. 6).

The first run was done using the typical power wheelchair manual joystick control (blue-dotted path in Fig. 6) to record for comparison the way this course would likely be navigated by a user able to control the joystick. The test run then allowed the automated navigation system to operate (red path in Fig. 6), with manual commands provided only to tell it to go at the start, and later to stop, rotate left, and move forward again so that the long corridor path could be selected. This 5-minute test was conducted 10 times for repeatability. The main obstacles were a cleaner's trolley and rubbish bin (static) and a person walking in the opposite direction (dynamic). Results in all cases were positive with consistently smooth passing of corridors at an average of 2.5km/h and the potential collisions with both static and dynamic obstacles were safely avoided in all cases.

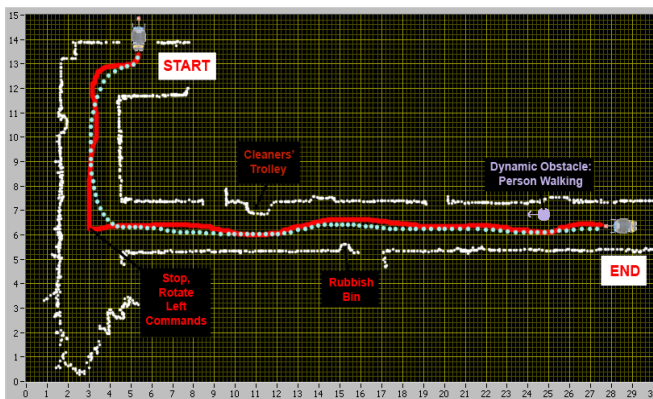


Fig. 6: System Performance Test at the Ryde Royal Rehab Centre

IV. CONCLUSION

This system has shown that the unique combination of both stereoscopic cameras and spherical vision cameras can be used to allow a semi-autonomous wheelchair to assist the user with effective guidance assistance when navigating in unknown indoor environments. The equine-inspired vision combination allows for both static objects and environmental attributes to be mapped as well as dynamic obstacles such as people walking past to be detected. The GUI also allows this system to provide more vision directly to the user through the camera streams being visible on screen. Automated navigation and obstacle avoidance strategies allow the safe maneuvering of the wheelchair throughout these environments, whilst avoiding collisions with both the static and dynamic obstacles from all angles.

This system will soon be combined with hands-free wheelchair control technology, in particular a brain-computer interface. The upcoming experimental trials to be conducted at the RRC will see the users communicate commands to the wheelchair with the hands-free controls, and the wheelchair carry out the commands whilst avoiding collisions and assisting with the safe navigational guidance.

REFERENCES

- [1] A. Mihailidis, P. Elinas, J. Boger, and J. Hoey, "An Intelligent Powered Wheelchair to Enable Mobility of Cognitively Impaired Older Adults: An Anticollision System", *IEEE Transactions on Neural Systems and Rehabilitation Engineering*, vol. 15, pp. 136-143, 2007.
- [2] R. A. Cooper, M. L. Boninger, D. M. Spaeth, D. Ding, G. Songfeng, A. M. Koontz, S. G. Fitzgerald, R. Cooper, A. Kelleher, and D. M. Collins, "Engineering Better Wheelchairs to Enhance Community Participation", *IEEE Trans. on Neural Systems and Rehabilitation Eng.*, vol. 14, pp. 438-455, 2006.
- [3] C. Galindo, J. Gonzalez, and J. A. F-Madrigal, "Control Architecture for Human-Robot Integration: Application to a Robotic Wheelchair", *IEEE Trans. on Systems, Man, and Cybernetics*, pp. 1053-1067, 2006.
- [4] A. Lankenau, and T. Rofer, "A versatile and safe mobility assistant", *IEEE Robotics and Automation Magazine*, vol. 8, pp. 29-37, 2001.
- [5] R. C. Simpson, D. Poirot, F. Baxter, "The Hephaestus Smart Wheelchair System", *IEEE Trans. on Neural Systems and Rehab. Eng.*, vol. 10, no. 2, 2002.
- [6] S. P. Levine, D. A. Bell, A. J. Lincoln, R. C. Simpson, Y. Koren, J. Borenstein, "The NavChair Assistive Wheelchair Navigation System", *IEEE Transactions on Rehabilitation Engineering*, vol. 7, no. 4, 1999.
- [7] P. Dario, M. C. Carrozza, L. Beccai, C. Laschi, B. Mazzolai, A. Menciassi, and S. Micera, "Design, fabrication and applications of biomimetic sensors in biorobotics", *Proceedings of the IEEE International Conference on Information Acquisition*, pp.263-266, 2005.
- [8] J. Murphy, C. Hall, and S. Arkins, "What Horses and Humans See: A Comparative Review", *Hindawi Corporation Internal Journal of Zoology*, 2009.
- [9] D. A. Samuelson, "Ophthalmic embryology and anatomy", *Veterinary Ophthalmology*, K. N. Gelatt, pp. 3-119, Lea & Febiger, USA, 1991.
- [10] A. Hughes, "The topography of vision in mammals of contrasting life style: comparative optics and retinal organization", *Handbook of Sensory Phys. Volume VII/5: The Visual System in Vertebrates*, pp. 613-756, Springer, Germany, 1977.
- [11] A. M. Harman, S. Moore, R. Hoskins, and P. Keller, "Horse vision and an explanation for the visual behaviour originally explained by the 'ramp retina'", *Equine Veterinary Journal*, vol. 31, pp. 384-390, 1999.
- [12] S. M. Roberts, "Equine vision and optics", *The Veterinary Clinics of North America. Equine Practice*, vol. 8, no. 3, pp. 451-457, 1992.
- [13] S. M. Crispin, A. G. Matthews, and J. Parker, "The equine fundus - I: examination, embryology, structure and function", *Equine Veterinary Journal. Supplement*, vol. 10, pp. 42-49, 1990.
- [14] P. McGreevy, *Equine Behaviour: A Guide for Veterinarians and Equine Scientists*, Saunders, UK, 2004.
- [15] J. S. Nguyen, T. H. Nguyen, and H. T. Nguyen, "Semi-autonomous Wheelchair System Using Stereoscopic Cameras", *31st Annual International Conference of the IEEE Engineering for Medicine and Biology Society*, pp. 5068-5071, 2009.
- [16] J. S. Nguyen, S. W. Su, and H. T. Nguyen, "Spherical Vision Cameras in a Semi-autonomous Wheelchair System", *32nd Annual International Conference of the IEEE Engineering for Medicine and Biology Society*, pp. 4064 - 4067, 2010.
- [17] J. Gong, Y. Duan, Y. Man, and G. Xiong, "VPH+: An Enhanced Vector Polar Histogram Method for Mobile Robot Obstacle Avoidance", *Proceedings of the 2007 IEEE Conference on Mechatronics and Automation*, pp 2784-2788, 2007.